Journal of Visualization, Vol. 10, No. 1 (2007)91-98

Visualization of Developing High Temperature Supersonic Impulse Jet Induced by Blast Wave Simulator

Mizukaki, T.*

* The First Research Center, Technical Research and Development Institute, Japan Defense Agency, Naka-Meguro, Meguro, Tokyo 153-8630, Japan. (Current affiliation: Dept. of Aeronautics and Astronautics, School of Engineering, TOKAI University, 1117 Kitakaname, Hiratsuka, Kanagawa 259-1292, Japan) E-mail: mizukaki@keyaki.cc.u-tokai.ac.jp

Received 25 August 2006
Revised 1 November 2006

Abstract: In order to investigate the developing characteristics of a high temperature supersonic impulse jet under an atmospheric ambient condition, we generate jets induced by an incident shock wave at Mach number 2.89, emerging from the open end of a high enthalpy blast wave simulator (HEBS). Developing high temperature supersonic impulse jets were visualized by the direction-indicating color schlieren method and analyzed by numerical calculations. A comparison of the experimental results with literature shows that the unsteady boundary area generated by the HEBS, starts to grow in half the time that the unsteady boundary area needs after the incident shock wave emerges in the literature.

Keywords: Flow visualization, Supersonic jet, Vortex, Blast wave, Shock tube.

1. Introduction

At the launch moment of a projectile by an acceleration device using propellant such as gun powder, the expulsion of propellant gases from the open end of its launch tube—muzzle— produces a strong impulse jet with shock waves. This jet is called a blast wave, and it expands symmetrically about the gun tube axis. From the viewpoints of both the projectile flight stability at the initial stage of ejection and the environmental evaluation of the blast wave, the studies on supersonic unsteady impulse jet play an important role. The optical flow visualization technique is a powerful experimental method to observe a supersonic flow field. The Schlieren method allows us to obtain the density gradient information of the interested flow by gray-scale images, but it needs a transparent medium condition (Merzkirch, 1987; Settle, 2001). The gases emerging from the muzzle of a single-stage powder gun, however, contain heavy smoke, numerous particles, and flames generated by uncombusted propellant gases; this prevents visualization of the flow field (Merlen and Dyment, 1995). Schmidt (Schmidt and Shear, 1975; Schmidt et al., 1984) has reported that the structure of the flowfield formed about the muzzle of a small caliber rifle during the firing by using a time-resolved, spark shadow-graph technique. Very near riegion of the muzzle, however, were not clearly visualized due to smoke of the propellant gas. Due to experimental difficulties of the ballistic research using large caliber guns, there have been many studies of numerical simulation on the blast wave development interaction. Most of them, however, has employed the overpressure profile around the muzzle as the evaluation value due to the difficulties of visualization of flow field (Cayzacr and Carette, 2000;

Crowley, 2000). Although Jiang have reported the interaction between an ejected high-speed projectile and emerging jet at the muzzle in detail by numerical simulation (Jiang and Takayama, 1998), little has been reported about comparison of the visualized flow field with the calculated one near the muzzle. In order to observe the characteristics of an unsteady impulse jet, numerous studies have examined the flow emerging from the open-end of a shock tube. Most of the reports describing the flow evolution have obtained their experimental results by using an incident shock Mach number of up to 2 (Elder and De Haas, 1952; Baird, 1987; Minota, 1993; Brouillette et al., 1995). Theoretically, an incident shock Mach number of more than 2.07 is needed to generate a supersonic impulse flow following an incident shock wave. A 20-mm caliber gun as an example of single-stage powder guns generates pressure that is more than 27 times higher than the atmospheric pressure and a temperature of approximately 1500 K at the muzzle (Baur and Schmidt, 1985). The pressure ratio is equal to that capable of generating an incident shock wave propagating at Mach 5 (Liepmann and Roshko, 1957). In order to replicate the phenomena generated by powder gun firing in the laboratory, the high temperature supersonic impulse jet to be examined needs to be driven by an incident shock wave propagating at more than Mach 2.07. Therefore, for an investigation on the developing blast wave characteristics, the incident shock wave needs to have a Mach number of more than 2.07. Then, we designed and assembled a high enthalpy blast wave simulator (HEBS) that has the ability to generate a high temperature supersonic impulse jet with a high Mach number from the open end of the launch tube.

In the present paper, as a fundamental study on developing blast waves for the improvement of projectile flight stability, both flow visualization and numerical analysis of high temperature supersonic impulse jets emerging from the open end of the HEBS have been carried out to confirm the difference between the jet developed by the HEBS and the reported experiment under similar conditions. Initially, a developing high temperature supersonic impulse jet induced by an incident shock wave with Mach 2.89 is visualized by the direction-indicating color schlieren method (DInCS). Later, the numerical analysis is carried out to identify structure of the jet in detail by using the commercial hydrocode AUTODYN-2D. Finally, both the development of a vortex ring and the unsteady boundary are confirmed by comparing them with the literatures.

2. Experimental Method

2.1 High Enthalpy Blast Wave Simulator

An experimental facility called the Transitional Ballistic Facility (TBSF) (Hisajima, 1999) located at the First Research Center, Technical Research and Development Institute (TRDI), Japan Defense Agency, has been employed to generate high temperature supersonic impulse jets. The TBSF has been assembled to investigate the dynamic phenomena around a projectile ejected into the air from the muzzle of a large caliber single-stage powder gun without disturbances such as smoke and flame that prevent optical observation (Nasuno, 2003). This facility can be divided into three sections: a high enthalpy blast wave simulator (HEBS), blow-down-type supersonic wind tunnel with a double diaphragm, and test section. The TBSF allows the simulation of transitional ballistic phenomena by shooting a projectile downwards through a generated blast wave against a supersonic wind blowing upwards.

Figure 1 shows a schematic diagram of the HEBS. The HEBS has the ability to launch a projectile by inserting it into the loading section equipped at the middle of the launch tube. The HEBS, which has a structure similar to that of an ordinary free-piston shock tube, consists of a high pressure tank equipped with an electromagnetic quick valve allowing the release of high pressure air up to 3.0 MPa within 1 ms and a 70-mm inner diameter compression tube with a length of 5.5 m. The shock tube is divided into two sections with a projectile loading section between them. The upstream section of the shock tube, the “primary shock tube”, is connected to a side of the projectile loading section, while the downstream section, the “acceleration tube”, is connected to the bottom of the

section. Hence, the acceleration tube is directed downwards from the projectile loading section into a test section. The vertical arrangement provides for a shot against the supersonic wind blowing upwards. Due to the force balance between the inertia of the projectile and the drag force, the projectile shot into the flow allows the observation of the free-flight projectile for approximately 350 ms. Note that the HEBS was only used to produce blast waves in the present experiments. The test section consists of a circular frame with an inner diameter and height of 1 m and 1.5 m, respectively. The section is equipped with four 500 mm diameter optical windows (BK7). Details of the design and operation procedure of the HEBS are described in the literature (Mizukaki and Arisawa, 2004). Table 1 shows the flow characteristics generated by the HEBS.

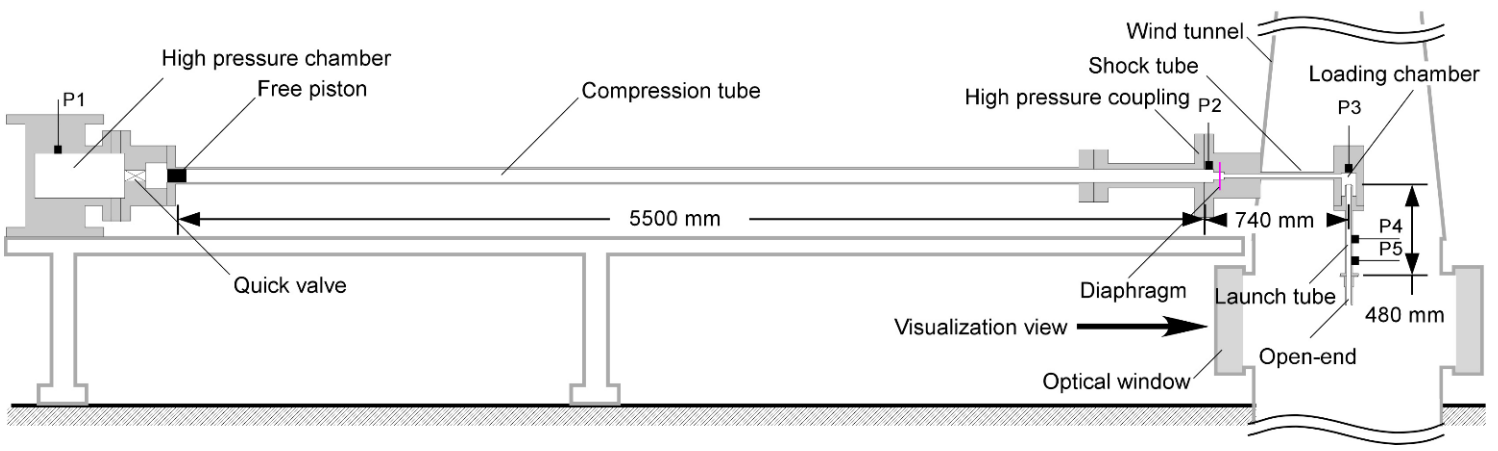

Fig. 1. Schematic diagram of the HEBS. P1, P2, P3, P4, P5: pressure gauges.

Table 1. Characteristics of supersonic-pulsed jet generated by HEBS.

Flow			Properties
Incident shock wave	Mach number	Ms	2.89
Test gas (Driven gas)	Velocity	U_1	0 m/s
	Pressure	P_1	0.1 MPa
	Temperature	T_1	288 K
Hot gas (Shock-induced flow)	Velocity	U_2	721 m/s
	Pressure	P_2	0.958 MPa
	Temperature	T_2	735 K
	Mach number	M_2	1.33
	Duration	δt	1 ms

2.2 Visualization Method

The DInCS (Kleine and Grönig, 1991) was used for identifying the density field. Figure 2(a) shows the optical alignment of the DInCS used for this experiment. The DInCS allows us to obtain a two-dimensional density gradient of the interested flow field with direction-indicating color in the obtained image. The DInCS acts as a powerful measurement technique for a complicated flow such as the blast wave.

The setup used here corresponds to the classic Toepler-Z configuration although with two exceptions. In a usual black-and-white configuration, the lens system behind the spark light source creates an image of the spark in the source plane (the focal plane of the first spherical mirror), while in this setup, the lenses are adjusted such that the spark light uniformly illuminates a colored filter source mask situated in that source plane. This is equivalent to forming a set of approximate point

light sources, each of which will produce a parallel light beam in its own color. The individual beams mix to form the parallel light beam traversing the test section. The separation into its components is carried out by the second spherical mirror, which refocuses the collimated beam, creating an inverted same-sized image of the source mask in its focal plane (focal length of both spherical mirrors: 5000 mm). An iris diaphragm serves as the schlieren stop, cutting off all beams but one. The light that is thus admitted to the film without any refraction in the test section produces the background color. Any change in the refractive index along the optical path leads to the displacement of the images of the colored sectors at the schlieren stop, causing other colors to appear on the film. The mixing of the colors will yield yellow, blue-green, and violet in different shades next to the basic colors—red, blue, and green.

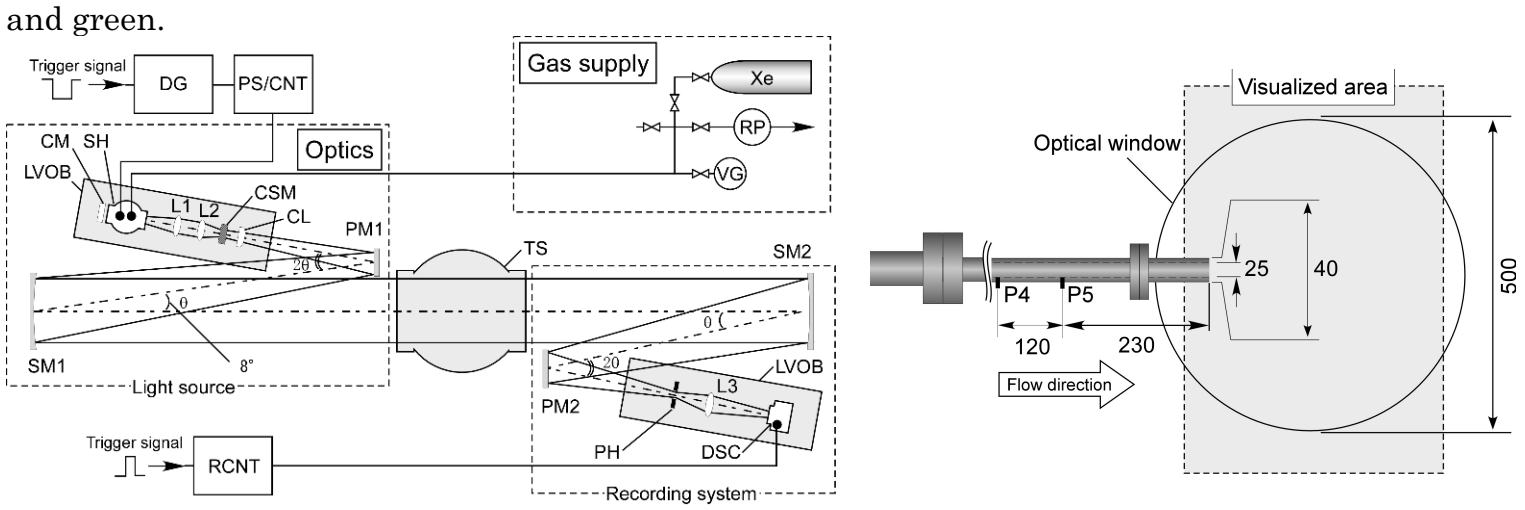

(a) (b)

Fig. 2. Schematic diagram of the DInCS. DG: Digital delay generator, PS/CNT: Power supply, SH: Spark head, CM: Concave mirror, L: Lens, CSM: Color source mask, CL: Cylindrical mirror, PM: Parabolic mirror, SM: Schlieren mirror, TS: Test section, PH: Pin hole, DSC: Digital still camera (unit: mm).

The light source for the color picture is a Xe-filled flash lamp (NANO-SPARK, NS-4000P, BIOLEK). With a spark duration of about 800 ns FWHM, the light output is sufficiently high to expose a charge-coupled device (CCD) inside a digital still camera (4024 by 1324 pixels, Nikon D1x).

Figure 2(b) shows the test section configuration. The cross-section of the launch tube is circular, with an inner and outer diameter of 25 mm and 40 mm, respectively. The pressure history produced by a blast wave inside the launch tube was obtained by pressure transducers (PCB Model 113B50) P4 and P5, which were located at a distance of 350 mm and 230 mm from the open end, respectively. The diameter of the optical window was 500 mm, while the hatched area was visualized.

2.3 Numerical Simulation

For a theoretical interpretation of the experimental results, numerical simulations were performed by the commercial hydrocode AUTODYN-2D (Century Dynamics, 1997) on a SGI workstation at the Computation Center of TRDI. The Euler equations for an axially symmetric pulsed flow were solved by a finite-difference flux-corrected Transport (FCT) scheme. The mesh number was 500 by 700 for a physical area of 125.0 mm by 187.5 mm. An implicit method was employed as the time integral method.

The computational domain used is shown in Fig. 3. On the outer boundary and downstream boundary, an ambient gas condition is applied: $(p, \rho, u, v) = (p_1, r_1, 0, 0)$, where ρ is the gas density; u, is the axial velocity; and v is the radial velocity of the gas flow. The initial condition of the test gas was set to be the standard atmosphere condition at sea level. On the walls of the muzzle model, BC, CD, DE and the jet axis, a symmetric condition is applied. On the upstream boundary inside the muzzle, a shock condition $(p, \rho, u, v) = (p_2, \rho_2, u_2, 0)$ is applied, where the quantities denoted by subscript 2 are obtained through the Rankine-Hugoniot relations for a specified shock Mach number $M = 2.89$. Corresponding to the experiments, the length CD was set to be 30 meshes and EF to be 50 meshes. Based on the numerical analysis (Ishii et al., 1999), the distance of the boundary from F was

set to be ten times the length of EF for the vertical direction and fifteen times for the horizontal direction. Therefore, the size difference between the computational domain and the test section affects the analysis result negligibly, even if they do not coincide with each other. Moreover, in this paper, a square mesh with a 0.25-mm interval was employed so that the non-dimensional mesh size (Δx, Δy) was set as (0.020, 0.025), while Ishii et al. have set the size as (0.05, 0.05). Here, Δ x and Δy represent the horizontal and vertical distance divided by the radius of the open end, 12.5 mm.

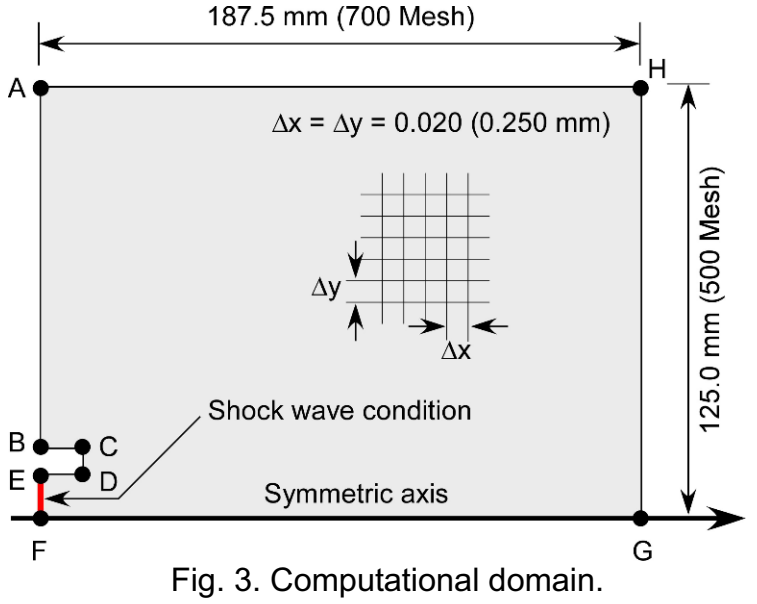

Fig. 3. Computational domain.

3. Results and Analysis

Golub (Golub, 1994) explains the development of a high temperature supersonic impulse jet by dividing the development process into three stages: in the first stage, the Mach number of the starting wave is larger than unity. The second stage is defined by the presence of large-scale vortex structures in the jet and the last stage is characterized by a quasi-steady gas flow. The first and the second stages of the present experiment are described below.

3.1 Blast Development at First Stage

In Fig. 4, the general features of a high temperature supersonic impulse jet produced by an incident shock wave with Ms = 2.89 emerging from the open end of the launch tube can be seen by both DInCS photographs (upper half) and calculated density contour maps (lower half).

Figure 4(a) shows the geometrical alignment of the muzzle in the images shown, including the image of a concave lens taken by the DInCS, with a long focal length of 10 m, and a diameter of 30 mm, as a reference image for helping to determine the direction of the density gradient by color. The digits in each figure show the elapsed time from the incident shock wave emerging from the muzzle, normalized by $t/(\gamma^{0.5} d/a_0)$, where t, γ, d, and a_0 are time, the specific ratio of air, inner diameter of the open end, and speed of sound in the ambient air, respectively.

Figure 4(b), at t' = 1.09 after the shock wave exited the open end, shows the flow-generating shock wave that is curved and weakened due to diffraction and geometrical attenuation. The jet already had a Mach disc (Sb) and barrel shock (Sc) following the contact surface (C). The reflected shock wave (Sd) had already developed from the triple point produced by Sb and Sc. At t' = 1.77 (Fig. 4(c)), the primary vortex (4) induced by the instability of the jet boundary was observed, and it continued to develop. At t' = 2.45 (Fig. 4(d)), the secondary vortex (5) was observed, while the primary vortex induced weak shock waves (Se) both ahead and behind its traveling direction. At t' = 3.13 (Fig. 4 (e)), Se developed and were clearly observed in both the DInCS image and the density contour map. At t' = 4.35 (Fig. 4(f)), the secondary vortex (5) developing simultaneously had propagated to approximately five times the distance of the diameter of the open end.

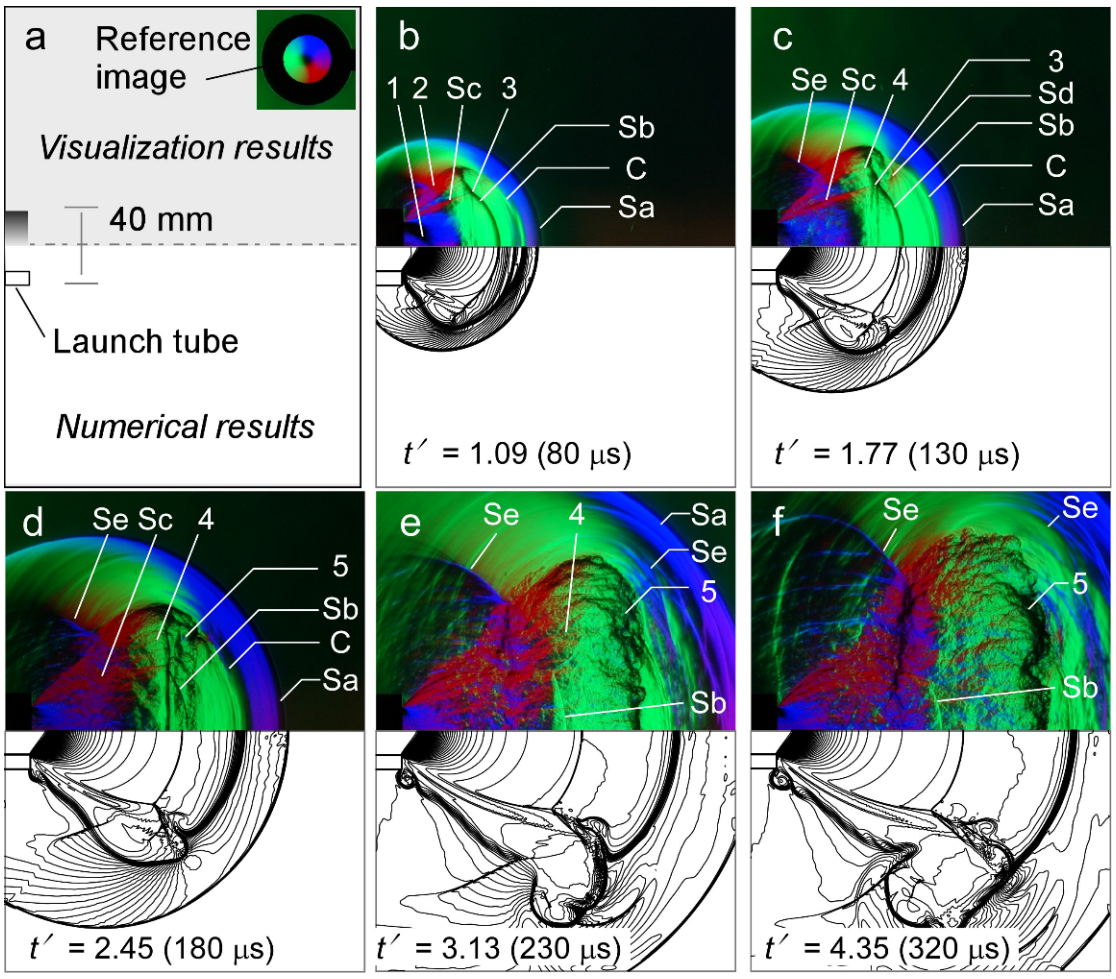

Fig. 4. Evolution of shock-wave-induced supersonic unsteady impulse jet under the ambient atmospheric condition at the muzzle. Sa: Incident shock wave, Sb: Mach disc, Sc: Barrel shock, Sd: Reflected shock wave, Se: Vortex-induced weak shock wave, 1: Expansion fan, 2: Jet boundary, 3: Triple point, 4: Primary vortex, 5: Secondary vortex.

3.2 Blast Development at Second Stage

The second stage of the development can be seen in Fig. 5. Due to existence of a temperature difference of approximately 450 K between the jet and ambient air, the second stage of the development is characterized by the appearance of a so-called “cocoon” structure generated between the head vortex of the jet and the launch tube. Figure 5(a) depicts the structure of the second stage. Figures 5(b), (c) and (d), show a head vortex (4) in the front part. Being a purely unsteady element of the jet structure, vortex (4) determines the dynamics of the impulse jets. Behind vortex (4), we have a jet flow with an unsteady boundary (3) and the initial part with a “barrel” structure (2). The unsteady boundary (3) is characterized by a noticeable broadening of the jet. The broadened unsteady boundary (3) is the cocoon, whose size is three times larger than the transverse size of the steady jet.

There exists much literature on the development of the vortex ring emerging from a shock tube. The reports on the development with supersonic jet, however, are sparse because the speed of the incident shock wave is needed Mach 2.07, at least, to generate the supersonic jet from the open end with the vortex. Figure 6 illustrates the time dependencies of the front and tail boundaries of the head vortices and cocoon, compared with the literature (Golub, 1994; Ishii, et al., 1999). Both of the literature has reported on the development of the vortex ring with supersonic jet. The conditions of each the experiments are shown in Table 2, where P_0, P_∞, T_0, T_∞, Ms, d, and Re are the stagnation pressure, ambient pressure, stagnation temperature, ambient temperature, incident shock Mach number, diameter of the open end, and the Reynolds number, respectively. In Fig. 6, the solid, dashed, and broken lines correspond to the results of the present experiment, and the literature, respectively. In the figure, W and W' is the region occupied by cocoon, and Z and Z' are those by the head vortex of

the jet. Only for the result by Ishii et. al., the trajectory of unsteady jet boundary is shown due to limited observation data. As shown here, the result by Ishii et. al is inferred to be same trajectory as the present experiment. The comparison between the result by the present experiment and by Golub indicates that a similar development tendency-the expansion of the region occupied by the vortex motion and the fixed tail boundary of the cocoon- were observed, whereas the cocoon appeared twice as earlier than that in the literature. The author infer that the Reynolds number affects the development of both jet and vortex structure at supersonic speed and that increasing the Reynolds number increases the speed of the development of vortex.

Table 2. Experimental conditions.

	P_0/P_∞	T_0/T_∞	P_∞ (kPa)	Ms (-)	d (mm)	$Re \times 10^{-6}$ (-)	Open end shape
Present paper	9.58	2.55	101 (atmospheric ambient condition)	2.89	25	1.19	Circular tube
Golub (1994)	10	4	Sub-atmospheric Pressure	3.09	20	1.02	Sonic nozzle at semi-infinite wall
Ishii et. al. (1999)	11	2.62	101	2.60	4	0.163	Circular tube

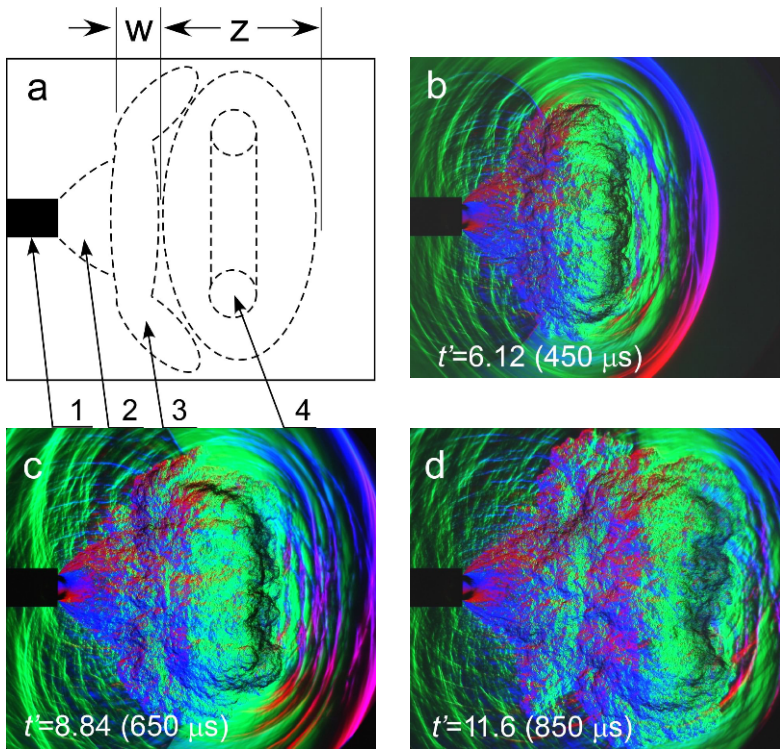

Fig. 5. DInCS images of the supersonic unsteady impulse jet under the atmospheric condition at the second stage: 1: launch tube, 2: initial part with a “barrel” structure, 3: unsteady jet boundary, 4: head vortex of the jet.

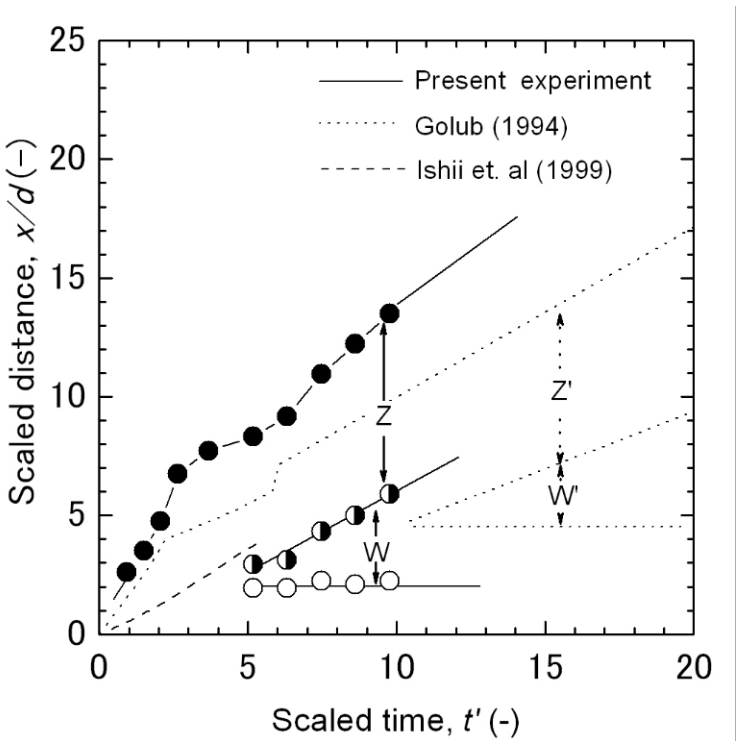

Fig. 6. Time dependencies of the region occupied by the vortices.

4. Conclusion

The flow visualization and numerical analysis of a developing high temperature supersonic impulse jet, in an atmospheric ambient condition, induced by a Mach 2.89 incident shock wave emerging from a circular open end by using high enthalpy blast wave simulator (HEBS) has been conducted. By

using the direction-indicating color schlieren method for the flow visualization, the results clearly show the structure of the jet in detail. The results of the numerical analysis agree well with the visualized images showing the structure of the inside of the jet in detail. The comparisons of the results obtained here with those reported by Golub, indicates that the absolute value of the ambient pressure have effect on the developing speed of the jet. We should take the absolute value of the ambient pressure into account for accurate assessment of the interaction between the jet and the projectile launched from a single-stage powder gun. In the present paper, only the experiment without projectile launch has been carried out. The further experimental and theoretical work on the interaction between the projectile and the jet is needed.

Acknowledgement

I wish to thank Dr. Harald Kleine of University of New South Wales/Australian Defence Force Academy for his kindness in reading, and commenting on, this paper.

References

Baird, J. P., Supersonic vortex rings, Proc. R. Soc. Lond. A, 409 (1987), 59-65.
Baur, E. H. and Schmidt, E. M., Relation ship between efficiency and blast from gas dynamic recoil brakes, Proceedings of AIAA 18th Fluid Dynamics and Plasmadynamics and Lasers Conference (Cincinatti, Ohio), (1985), AIAA-85-1718.
Brouillette, M., Tardif, J. and Gauthier, E., Experimental study of shock-generated vortex rings, Shock Waves @ Marseille (ed. R. Brun and L. Z. Dumitresu), (1995), 361-366, Springer-Verlag.
Cayzacr, R. and Carette, E., Intermediate ballistic and aeroballistics overview and prespectives, Proceedings of European Forum on Ballisrtc of Projectiles (Saint-Louis, France), (2000), 259-274,
Century Dynamics, AUTODYN electronic document Library, (1997), Century Dynamics,
Crowley, A. B., Muzzle flow field evolution, Proceedings of European Forum on Ballistics of Projectiles (Saint-Louis, France), (2000), 241-247,
Elder, F. K. J. and De Haas, N., Experimental study of the formation of a vortex ring at the open end of a cylindrical shock tube, Journal of Applied Physics, 23-10 (1952), 1065-1069.
Golub, V. V., Development of shock wave and vortex structures in unsteady jets, Shock Waves, 3 (1994), 279-285.
Hisajima, S., Outline of transition ballistic simulation facility, Defense Technology Journal, 19-6 (1999), 4-12.
Ishii, R., Fujimoto, H., Hatta, N. and Umeda, Y., Experimental and numerical analysis of circular pulse jets, J. Fluid Mech., 392 (1999), 129-153.
Jiang, Z. and Takayama, K., Numerical study on blast flowfields induced by supersonic projectiles discharged from shock tubes, Phys. Fluids, 10-1 (1998), 277-288.
Kleine, H. and Grönig, H., Color schlieren methods in shock wave research, Shock Waves, 1 (1991), 51-63.
Liepmann, H. W. and Roshko, A., Elements of gasdynamics, (1957), John Wiley & Sons, New York.
Merlen, A. and Dyment, A., Similarity and patterns for non-instantaneous explosions, Shock Waves @ Marseille (ed. R. Brun and L. Z. Dumitresu), (1995), 393-398.
Merzkirch, W., Flow visualization, (1987), Academic Press.
Minota, T., Interaction of a shock wave with a high-speed vortex ring, Fluid Dynamic Research, 12 (1993), 335-342.
Mizukaki, T. and Arisawa, H., Visualization of gun muzzle balst wave using direction-indicating color schlieren method, Technical Report 6852, Technical Research and Development Institute, Japan Defense Agency, (2004).
Nasuno, Y., Study on transitional ballistic simulation technology, Defense Technology Journal, 23-6 (2003), 24-31.
Schmidt, E. M., Gordnier, R. E. and Fansler, K. S., Interaction of gun exhaust flowfield, AIAA Journal, 22-4 (1984), 516-517.
Schmidt, E. M. and Shear, D. D., Optical measurement of muzzle blast, AIAA Journal, 13-8 (1975), 1086-1091.
Settle, G. S., Schlieren and Shadowgraph Techniques, (2001), Springer-Verlag, Berlin.

Author Profile

Toshiharu Mizukaki: He received his B Sc (Sc) in Physics in 1991 from the Tokyo University of Science. From 1991 to 1999, he worked in Japan Atomic Energy Agency (JAEA) as a scientist. He received his Ph.D. in Aerospace Engineering in 2001 from Tohoku University. He worked in NASA Langley Research Center as a visiting scientist in 2001, and in the Technical Research and Development Institute of Japan Defense Agency from 2002 to 2005. He has been working in the Department of Aeronautics and Astronautics, School of Engineering, TOKAI University, as an associate professor since 2006. His research interests are shock waves, high-speed launch system, flow visualization, and laser-applied measurement techniques.